NASA Contractor Report 172592

ICASE REPORT NO. 85-25

NASA-CR-172592
19850021315

ICASE

SHOCK CAPTURING

Stephen F. Davis

Contract No. NAS1-17070

April 1985

INSTITUTE FOR COMPUTER APPLICATIONS IN SCIENCE AND ENGINEERING
NASA Langley Research Center, Hampton, Virginia 23665

Operated by the Universities Space Research Association

National Aeronautics and
Space Administration

Langley Research Center
Hampton, Virginia 23665

SHOCK CAPTURING

Stephen F. Davis
Institute for Computer Applications in Science and Engineering

ABSTRACT

This chapter describes recent developments which have improved our understanding of how finite difference methods resolve discontinuous solutions to hyperbolic partial differential equations. As a result of this understanding improved shock capturing methods are currently being developed and tested. Some of these methods are described and numerical results are presented showing their performance on problems containing shocks in one and two dimensions.

We begin this discussion by defining what is meant by a conservative difference scheme and showing that conservation implies that, except in very special circumstances, shocks must be spread over at least two grid intervals. These two interval shocks are actually attained in one dimension if the shock is steady and an upwind scheme is used. By analyzing this case, we determine the reason for this excellent shock resolution and use this result to provide a mechanism for improving the resolution of two dimensional steady shocks. Unfortunately, this same analysis shows that these results cannot be extended to shocks which move relative to the computing grid.

To deal with moving shocks and contact discontinuities we introduce total variation diminishing (TVD) finite difference schemes and flux limiters. We show that TVD schemes are not necessarily upwind, but that upwind TVD schemes perform better because they permit a wider choice of flux limiters. The advantage of non-upwind TVD schemes is that they are easy to implement. Indeed, it is possible to add an appropriately chosen artificial viscosity to a conventional scheme such as MacCormack's method and make it TVD. We conclude by presenting some theoretical results on flux limiters and some numerical computations to illustrate the theory.

Research was supported by the National Aeronautics and Space Administration under NASA Contract No. NAS1-17070 while the author was in residence at ICASE, NASA Langley Research Center, Hampton, VA 23665.

1. Introduction

We wish to consider the numerical solution of hyperbolic systems of the form

$$\mathbf{u}_t + f(\mathbf{u})_x = 0, \ t > 0, \ -\infty < \mathbf{x} < \infty \tag{1.1}$$

where $\mathbf{u}(x,t)$ and $f(\mathbf{u}(\mathbf{x},t))$ are m-vectors.

In general, systems of this form admit discontinuous (shock) solutions which satisfy the Rankine-Hugoniot jump conditions

$$\mathbf{s}\,[\![\,\mathbf{u}\,]\!] = [\![\,f\,]\!] \tag{1.2}$$

where $[\![\,\mathbf{u}\,]\!]$ denotes the jump in the variable $\mathbf{u}$ across the shock and $\mathbf{s}$ is the speed of propagation of the shock.

In the following we consider finite difference schemes which can be put into the following conservation form

$$U_j^{n+1} = U_j^n - \frac{\Delta t}{\Delta x}\left[F_{j+1/2}^n\left(U_{j-k}^n, \ldots, U_{j+l}^n\right) - F_{j-1/2}^n\left(U_{j-1-k}^n, \ldots, U_{j-1+l}^n\right)\right] \tag{1.3}$$

because Lax and Wendroff [4] have shown that covergent schemes of the form (1.3) converge to solutions which satisfy equation (1.2). To show why these schemes are called conservative, we apply (5.2.3) to (1.1) with periodic boundary conditions and sum over one period. The result is

$$\sum_j U_j^{n+1} = \sum_j U_j^n \ ; \tag{1.4}$$

if we apply this result recursively, we obtain

$$\sum_j U_j^{n+1} = \sum_j U_j^0 \tag{1.5}$$

which says that the discrete integral of the solution is conserved. This conservation property implies that shocks which fall between mesh points can at best be represented by transitions over two intervals. That is, a shock of the form

$$\mathbf{u}(\mathbf{x}) = \begin{cases} \mathbf{u}_L, & \text{for } \mathbf{x} < \mathbf{x}_s \\ \mathbf{u}_R, & \text{for } \mathbf{x} > \mathbf{x}_s \end{cases} \tag{1.6}$$

where $\mathbf{x}_{j-1/2} < \mathbf{x}_s < \mathbf{x}_{j+1/2}$ can, at best, be represented by a transition of the form

$$U_i^n = \begin{cases} \mathbf{u}_L, & \text{for } i < j \\ \mathbf{u}_m, & \text{for } i = j \\ \mathbf{u}_R, & \text{for } i > j \end{cases} \tag{1.7}$$

where

$$\mathbf{u}_m(\mathbf{x}_{j+1/2} - \mathbf{x}_{j-1/2}) = \mathbf{u}_L(\mathbf{x}_s - \mathbf{x}_{j-1/2}) - \mathbf{u}_R(\mathbf{x}_{j+1/2} - \mathbf{x}_s)$$
$$\mathbf{x}_{j+1/2} = (\mathbf{x}_{j+1} + \mathbf{x}_j)/2 \tag{1.8}$$

satisfies (1.5). In most practical computations, shocks are spread over many more than two intervals. In this paper we examine why this is so and how shock resolution approaching that of equation (1.7) can be attained.

2. One Dimensional Steady Shocks

In this section we study the application of upwind difference schemes to the numerical computation of one dimensional steady shocks. We undertake this study not because this problem is of general interest but because it is known that upwind differences schemes attain two interval shock resolution in this case. By studying this case in detail we can determine which features of these schemes are responsible for this excellent shock capturing ability. In the next section we use this knowledge to construct shock capturing schemes for two dimensional steady shocks. Since this theory requires moving grids to capture moving shocks, we examine the moving shock problem from a different point of view in a later section.

To simplify the details we restrict this discussion to the scalar equation

$$u_t + f(u)_x \equiv u_t + a(u)u_x = 0,\ a(u) = \frac{df(u)}{du};\ t > 0,\ x_0 < x < x_N \tag{2.1}$$

and consider the first order upwind difference scheme of Murman and Cole [5]. This is a reasonable thing to do because modern high order methods are designed to become first order in the vicinity of shocks and because the Murman and Cole method can be extended to systems by a procedure developed by Roe [9].

Consider a partition of the x axis

$$x_0 < x_1 < \ldots < x_N \tag{2.2}$$

and locally linearize equation (2.1) on each interval (x_j, x_{j+1}). That is let

$$u_t + a(u_j, u_{j+1})u_x = 0 \tag{2.3}$$

where

$$a(u_j, u_{j+1}) = \begin{cases} \Delta f_j/\Delta u_j, & \text{if } \Delta u_j \neq 0 \\ df(u_j)/du, & \text{if } \Delta u_j = 0 \end{cases} \tag{2.4}$$

and $\Delta u_i = u_{i+1} - u_i,\ \Delta f_i = f_{i+1} - f_i$. If we define

$$a^+(u_j, u_{j+1}) = \max\,(0, a(u_j, u_{j+1})) \tag{2.5}$$

and

$$a^-(u_j, u_{j+1}) = \min\,(0, a(u_j, u_{j+1}))\,, \tag{2.6}$$

then we can write the Murman-Cole scheme in the form

$$U_j^{n+1} = U_j^n - \frac{2\Delta t}{(\Delta x_{j-1} + \Delta x_j)} \Big\{ a^+(U_{j-1}^n, U_j^n)\Delta U_{j-1}^n + a^-(U_j^n, U_{j+1}^n)\Delta U_j^n \Big\} \tag{2.7}$$

or in the alternative form

$$U_j^{n+1} = U_j^n - \frac{2\Delta t}{(\Delta x_{j-1} + \Delta x_j)} \left\{ \Delta f_{j-1}^+ + \Delta f_j^- \right\}. \tag{2.8}$$

This method can also be written in conservation form

$$U_j^{n+1} = U_j^n - \frac{2\Delta t}{(\Delta x_{j-1} + \Delta x_j)} \left\{ F(U_j^n, U_{j+1}^n) - F(U_{j-1}^n, U_j^n) \right\} \tag{2.9}$$

if we define

$$\begin{aligned} F(u_j, u_{j+1}) &= f(u_{j+1}) - \Delta f_j^+ \\ &= f(u_j) + \Delta f_j^- \\ &= 1/2\{f(u_j) + f(u_{j+1}) + \Delta f_j^- - \Delta f_j^+\} \end{aligned} \tag{2.10}$$

and note that

$$f(u_{j+1}) - f(u_j) = \Delta f_j^+ + \Delta f_j^-. \tag{2.11}$$

The main result of this section is the following theorem.

Theorem. Consider the following representation of a steady shock at time t^n

$$u_j^n = \begin{cases} u_L, & \text{for } j < 0 \\ u_m, & \text{for } j = 0 \\ u_R, & \text{for } j > 0 \end{cases} \tag{2.12}$$

where u_m is some intermediate value between u_L and u_R while u_L and u_R satisfy the steady Rankine-Hugoniot jump condition

$$f(u_R) - f(u_L) = 0 \tag{2.13}$$

and the geometric entropy condition

$$a(u_L) = \frac{df}{du}(u_L) > 0 > \frac{df}{du}(u_R) = a(u_R) \tag{2.14}$$

if u_m is such that

$$a(u_L, u_m) > 0 > a(u_m, u_R) \tag{2.15}$$

then (2.12) is a stable steady solution to (2.8).

Proof A direct calculation shows that equation (2.12) solves (2.8). That is:
for $j < -1$

$$\Delta f_j^+ = f(u_L) - f(u_L) = 0$$
$$\Delta f_j^- = 0 \text{ , since } a(u_L, u_L) = a(u_L) > 0$$

for $j \geq 1$

$$\Delta f_j^+ = 0 \text{ , since } a(u_R, u_R) = a(u_R) < 0$$
$$\Delta f_j^- = f(u_R) - f(u_R) = 0$$

for $j = -1$

$$\Delta f_{-1}^+ = f(u_m) - f(u_L)$$
$$\Delta f_{-1}^- = 0 \text{ , since } a(u_L, u_m) > 0$$

and for $j = 0$

$$\Delta f_0^+ = 0 \text{ , since } a(u_m, u_R) < 0$$
$$\Delta f_0^- = f(u_R) - f(u_m)$$

so

$$\begin{aligned}\Delta f_{-1}^+ + \Delta f_0^- &= f(u_m) - f(u_L) + f(u_R) - f(u_m) \\ &= f(u_R) - f(u_L) = 0.\end{aligned}$$

To prove stability assume that $u_j^n = u_L + e^n$ for some $j < -1$. Then

$$\begin{aligned}(u_L + e^{n+1}) &= (u_L + e^n) - \frac{\Delta t}{\Delta x}[f(u_L + e^n) - f(u_L)] \\ &= u_L + e^n - \frac{\Delta t}{\Delta x}[a(u_L)e^n + 0(e^n)^2] \\ &= (1 - a_L\frac{\Delta t}{\Delta x})e^n + 0(e^n)^2.\end{aligned}$$

Since

$$0 < a_L\frac{\Delta t}{\Delta x} < 1 \text{ , } 0 < (1 - a_L\frac{\Delta t}{\Delta x}) < 1$$

$e^{n+1} \to 0$ as $n \to \infty$ and the solution is stable.
A similar argument holds for $j > 1$. ∎

If we consider the conservation form of the scheme (2.9), (2.10), we note that the numerical fluxes

$$F(u_L, u_m) = f(u_L) \tag{2.16}$$

and

$$F(u_m, u_R) = f(u_R) \tag{2.17}$$

do not depend on the intermediate value u_m. If we study the pointwise error in the computed solution, we note that since u_m should have the value of either u_L or u_R, u_m is in error by order $(u_R - u_L)$. Equations (2.16), (2.17) trap this error at one grid point and prevent it from propagating through the domain. This is the property of the upwind methods which is responsible for their excellent ability to

capture steady shocks. Methods with a numerical flux that depend explicitly on u_m will create an error that will propagate throughout the domain of the calculation. This error will show up either as a spreading of the shock or as wiggles in the solution.

Unfortunately, if a shock moves through a grid, the computed solution at points left behind will depend on intermediate values such as u_m. Thus, it is not possible to avoid the propagation of error to points away from a shock when a shock moves relative to the computing grid.

3. Two Dimensional Steady Shocks

In the preceding section we showed how upwind differencing improves the resolution of steady one dimensional shocks. Here we extend these results to the two dimensional Euler equations of gas dynamics.

To show that more is needed than a straightforward application of the results of the last section, we consider the exact weak solution to the Euler equations which corresponds to a plane oblique shock. Such a solution can be constructed by superimposing an arbitrary tangential velocity on a one dimensional shock and choosing a cartesian coordinate system that is aligned with the upstream velocity vector (see Figure 1).

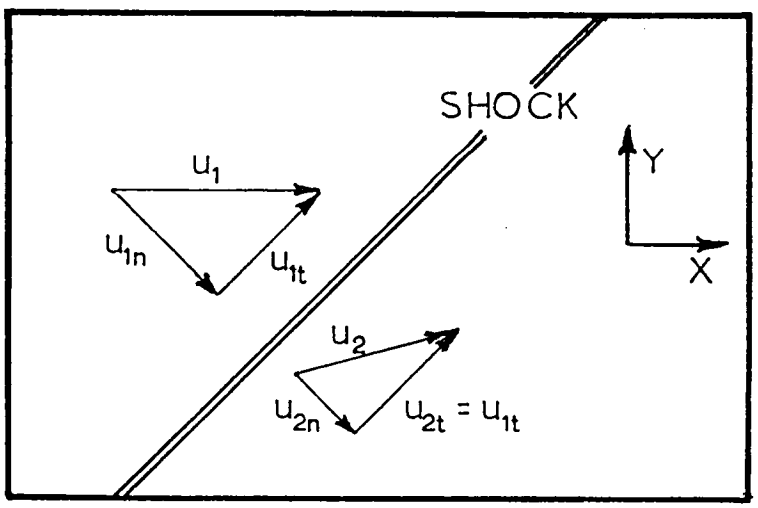

Figure 1. Plane oblique shock solution.

Before we continue, we note that for the Euler equations the direction of differencing for the x and y derivatives in an upwind scheme is determined by the local Mach numbers M_x and M_y, respectively, where

$$M_x = u/a, \; M_y = v/a, \; a = \sqrt{\gamma p/\rho} \tag{3.1}$$

and (u, v) are the components of the velocity vector $\mathbf{v}$ along the components (x, y) of the position vector $\mathbf{x}$. If $M_x > 1$, backward differences are used for all x derivatives. If $M_x < -1$, forward differences are used for all x derivatives. If $-1 < M_x < 1$, x derivatives are approximated by both forward and backward differences according to some recipe (cf., e.g., Osher[7], Roe[8], van Leer[12]). Corresponding rules hold for the y derivatives.

Returning to the oblique shock solution illustrated in Figure 1, we note that since the tangential velocity is arbitrary, it can be chosen large enough to make $M_x > 1$ on both sides of the shock. If this is done, the direction of differencing does not change across the shock, as it should. The method does not "see" the shock and the shock is spread as shown in Figure 2.

Other difficulties involve the differencing of derivatives in the direction tangent to the shock. We discuss these problems below.

One way to avoid these problems is to choose a computing grid which is aligned with the shock. This restores the one dimensional shock resolution. Unfortunately, it is very difficult to choose such a grid, especially when multiple shocks intersect. For this reason we pursue the alternative approach of deriving a method on an arbitrary grid which mimics the behavior of a method constructed on an aligned grid.

To carry this out, we write the Euler equations in a local coordinate system, (x', y') which is aligned with potential shock directions and is rotated with respect to the coordinate system of the computing grid (x, y). At this time we assume that these directions are known. This geometry is shown in Figure 3.

Since the Euler equations are invariant under rotation, they can be written immediately in the new coordinate system as

$$\frac{\partial \mathbf{w}'}{\partial t} = -\frac{\partial \mathbf{f}'(\mathbf{w}')}{\partial x'} - \frac{\partial \mathbf{g}'(\mathbf{w}')}{\partial y'} \tag{3.2}$$

where

$$\begin{aligned} \mathbf{w}' &= [\rho, \rho u', \rho v', e]^T \\ \mathbf{f}' &= [\rho u', \rho u'^2 + p, \rho u' v', (e+p)u']^T \\ \mathbf{g}' &= [\rho v', \rho u' v', \rho v'^2 + p, (e+p)v']^T \\ e &= p/(\gamma - 1) + 1/2\rho(u'^2 + v'^2) \end{aligned} \tag{3.3}$$

and

$$\begin{aligned} u' &= u\cos\theta + v\sin\theta \\ v' &= -u\sin\theta + v\cos\theta. \end{aligned} \tag{3.4}$$

If the coordinate system is aligned with a plane steady shock, the derivatives in the second term on the right of (3.2) would exist and be equal to zero. This reduces

the two-dimensional problem, locally, to the one-dimensional problem described in the previous section. By choosing different discretizations for each term on the right of (3.2), we attempt to construct a numerical scheme which mimics this behavior.

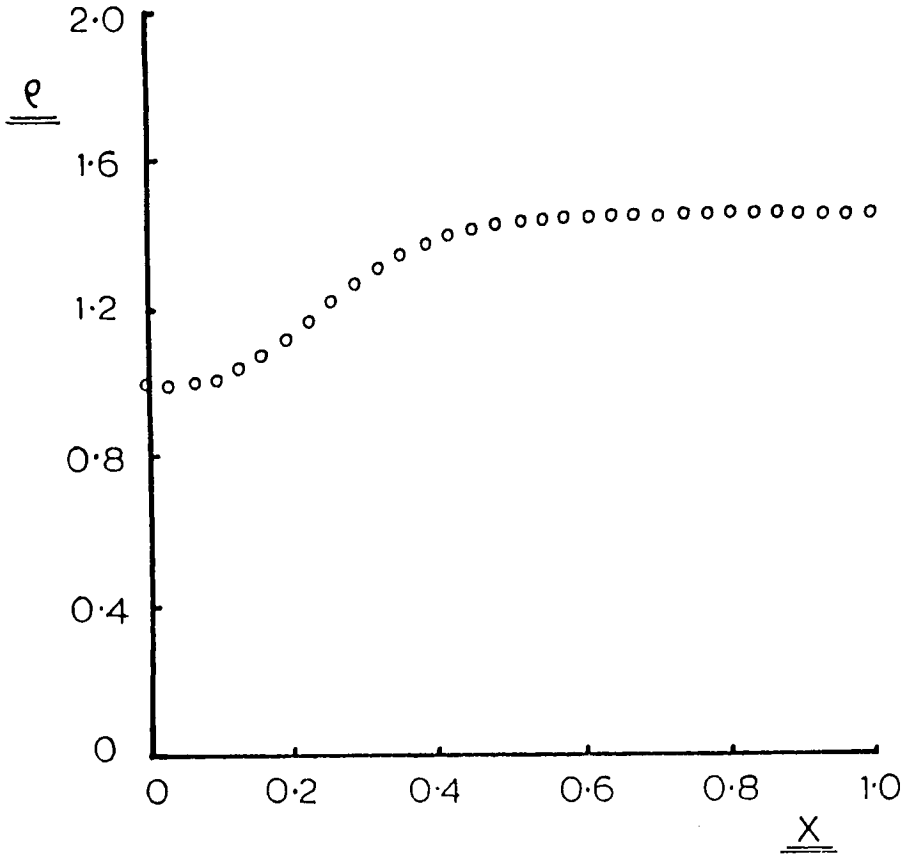

Figure 2. Density profile through an oblique shock computed using a first order upwind scheme.

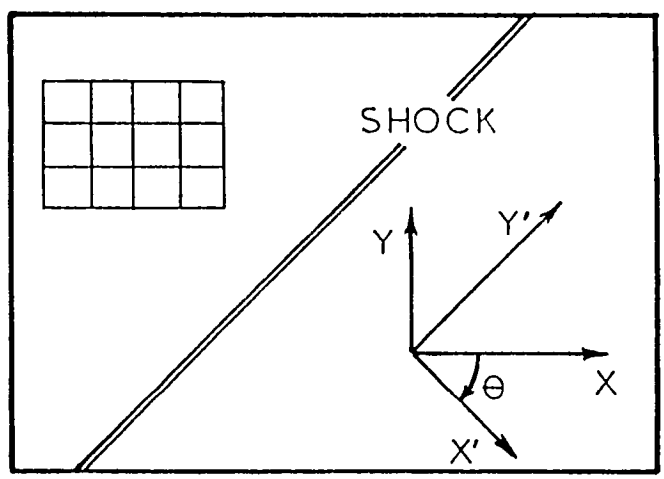

Figure 3. Geometry of local and global coordinate systems.

If we express the first term on the right of (3.2) in global coordinates, we get

$$\frac{\partial \mathbf{f}'}{\partial x'} = \cos\theta \frac{\partial \mathbf{f}'}{\partial x} + \sin\theta \frac{\partial \mathbf{f}'}{\partial y}. \tag{3.5}$$

This is approximated by the finite difference expression

$$\begin{aligned} &\frac{\cos\theta}{\Delta x}[F'(W'_{i,j}, W'_{i+1,J}) - F'(W'_{i-1,j}, W'_{i,j})] \\ &+\frac{\sin\theta}{\Delta y}[F'(W'_{i,j}, W'_{i,j+1}) - F'(W'_{i,j-1}, W'_{i,j})] \end{aligned} \tag{3.6}$$

where F' is an upwind numerical flux such as that described in section 2.3 and W' is the numerical approximation to $\mathbf{w}'$.

The second term on the right of (3.2) is the directional derivative of $\mathbf{g}'$ in the y' direction. If we write this expression in global coordinates we get

$$\frac{\partial \mathbf{g}'}{\partial y'} = -\sin\theta \frac{\partial \mathbf{g}'}{\partial x} + \cos\theta \frac{\partial \mathbf{g}'.}{\partial y} \tag{3.7}$$

when we attempted to approximate (3.7) on the usual five point stencil, the results were unacceptable regardless of the choice of numerical flux. This leads us to believe that an acceptable approximation to (3.7) must include the corner points (x_{i+1}, y_{j+1}) and (x_{i-1}, y_{j-1}). Therefore, we chose the discretization

$$\begin{aligned} &\frac{-\sin\theta}{\Delta x}[G'(W'_{i,j1(\theta)}, W'_{i+1,j2(\theta)}) - G'(W'_{i-1,j1(\theta)}, W'_{i,j2(\theta)})] \\ &+\frac{\cos\theta}{\Delta y}[G'(W'_{i1(\theta),j}, W'_{i2(\theta),j+1}) - G'(W'_{i1(\theta),j-1}, W'_{i2(\theta),j})] \end{aligned} \tag{3.8}$$

where the functions $j1, j2, i1$ and $i2$ are chosen so that the resulting stencil provides the closest possible approximation to the directional derivative. These functions are tabulated in Table 5.1 and the resulting stencils are shown in Figure 4. With this construction, the results did not seem to depend strongly on the choice of numerical flux although less dissipative numerical fluxes gave slightly better results than more dissipative numerical fluxes.

Case	Angle Range	j1	j2	i1	i2
a	$-\infty < \tan(\theta) < -\Delta x/\Delta y$	j	j	i-1	i+1
b	$-\Delta x/\Delta y < tan(\theta) < 0$	j-1	j+1	i	i
c	$0 < tan(\theta) < \Delta x/\Delta y$	j+1	j-1	i	i
d	$\Delta x/\Delta y < tan(\theta) < \infty$	j	j	i+1	i-1

Table 5.1 Definition of Computational Stencils.

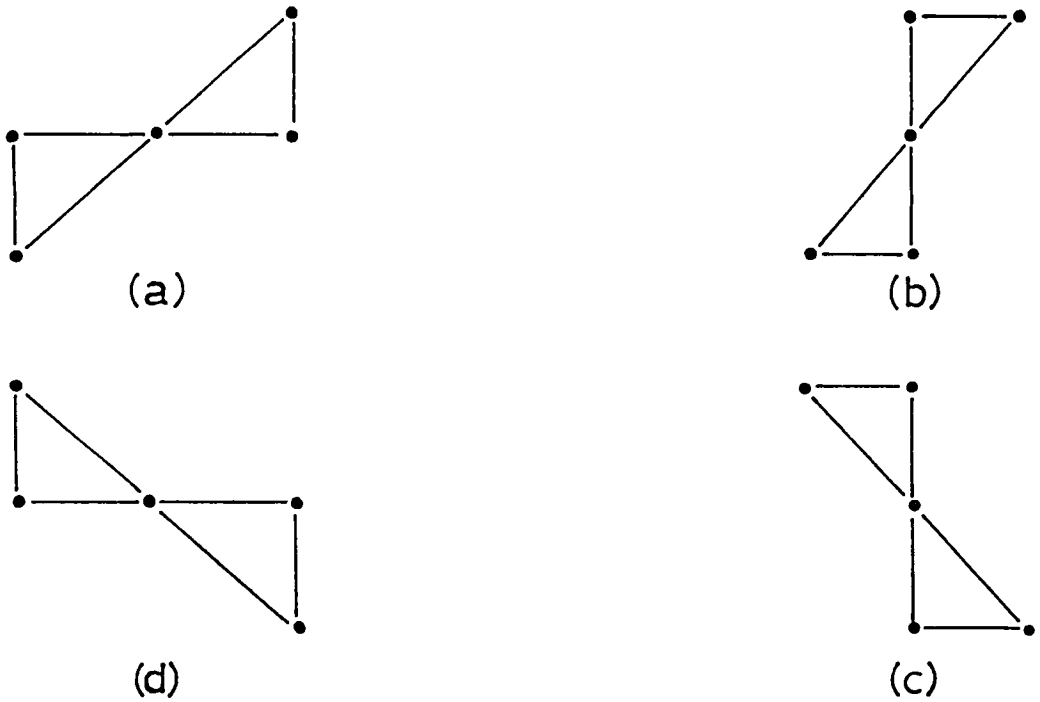

Figure 4 Computational stencils for tangential derivative approximations.

Expressions (3.6) and (3.8) have been derived under the assumption that we can associate a unique value of the angle θ with each computational cell. Unfortunately, it does not seem to be possible to allocate the angles in this way and still construct a conservative difference scheme. Therefore we have chosen to associate a value of the angle with each cell boundary. This permits us to construct the following conservative difference scheme

$$W_{i,j}^{n+1} = W_{i,j}^{n} - \frac{\Delta t}{\Delta x}\left[F_{i+1/2,j} - F_{i-1/2,j}\right] - \frac{\Delta t}{\Delta y}\left[G_{i,j+1/2} - G_{i,j-1/2}\right] \tag{3.9}$$

where cartesian tensor transformation rules are used to construct the numerical fluxes from the rotated numerical fluxes. That is, formula of the form

$$\begin{aligned} f_1(w) = \rho u &= \rho u' \cos\theta - \rho v' \sin\theta \\ &= f_1'(w') \cos\theta - g_1'(w') \sin\theta \end{aligned} \tag{3.10}$$

is used when f_1 is the flux of a scalar variable such as ρ or e and a formula of the form

$$\begin{aligned} f_2(w) &= \rho u^2 + p = \rho(u' \cos\theta - v' \sin\theta)^2 + p \\ &= \rho u'^2 \cos^2\theta - 2\rho u' v' \cos\theta \sin\theta + \rho v'^2 \sin^2\theta + p(\cos^2\theta + \sin^2\theta) \\ &= f_2'(w') \cos^2\theta - g_2'(w') \cos\theta \sin\theta - g_3'(w') \cos\theta \sin\theta + f_3'(w') \sin^2\theta \end{aligned} \tag{3.11}$$

is used when f_2 is the flux of a vector component such as ρu or ρv.

Finally, we show how the angles used in the algorithm are determined. We note in passing that we do not attempt to determine whether or not a shock actually exists. Instead the algorithm assumes that a shock exists between each pair of grid points and determines its orientation. This approach locates the proper direction when it is needed and causes no problems otherwise.

In reference [1], we determine the direction of the normal to a shock which is assumed to lie between two grid points as the direction of the jump in velocity between the grid points. This works well when the computing grid is uniform but fails when the grid is highly stretched. To overcome this problem we now determine the direction of a shock normal as the direction of the gradient of a scalar variable such as the pressure or density. Suitably smoothed numerical approximations to the gradient have provided proper shock angles in all cases that we have tried.

Figures 5 to 7 show the results of computations of a two dimensional shock reflection using the first order scheme of Osher, the second order scheme of van Leer, and the present scheme respectively. These figures clearly show that rotational bias considerably improves the shock resolution of first order schemes. Indeed the shock resolution of a first order accurate rotationally biased scheme rivals that of a sophisticated second order method.

In a first attempt to obtain a higher order rotational scheme, we replaced the first order numerical fluxes of the present method with second order numerical fluxes. The resulting scheme gave some improvement in shock resolution but was quite sensitive to the treatment of boundary conditions and was probably too complex to be of practical use. It is not clear that the small improvement in shock resolution over current second order methods would justify the considerable increase in complexity of the scheme. It is also not entirely clear that the resulting scheme is actually second order. For these reasons there is still need for research on high order two dimensional schemes.

4. TVD Finite Difference Schemes and Flux Limiters

The method described in the previous section is at this time only first order accurate and has been designed especially for problems with steady shocks. In this section, we examine second order methods which are designed to give good results when applied to problems containing moving shocks and contact discontinuities as well as steady shocks.

In order to demonstrate the main ideas in a simple setting, we consider here only the linear advection equation

$$u_t + a u_x = 0, \quad a = \text{ constant.} \tag{4.1}$$

The extension of this work to nonlinear equations, systems and multiple dimensions is described in reference [2].

We consider explicit finite difference schemes in conservation form which approximate equation (4.1) and which we denote by

$$U^{n+1} = L.U^n. \tag{4.2}$$

The total variation of a mesh function is defined by the formula

$$TV(U^n) = \sum_i |U^n_{i+1} - U^n_i| \tag{4.3}$$

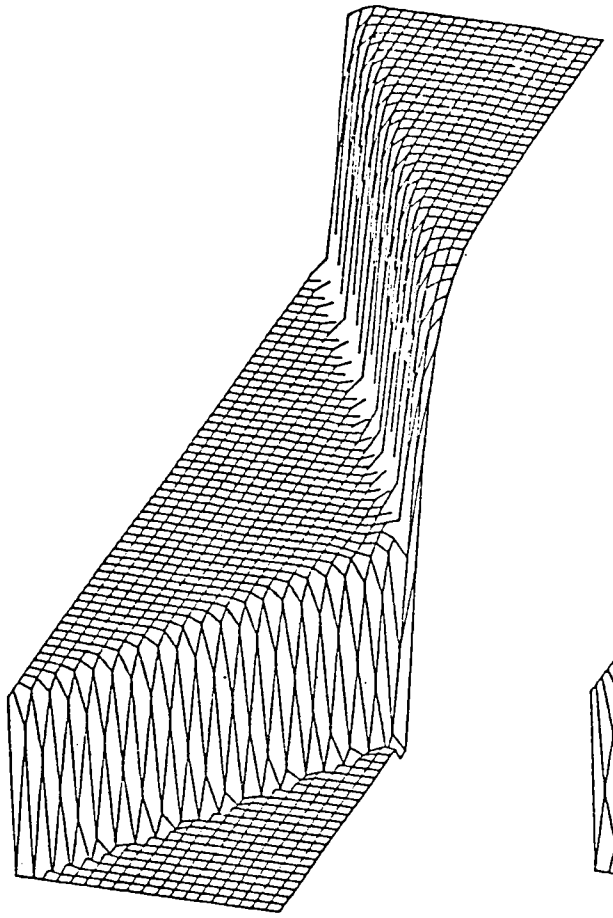

Figure 5 Three dimensional density plot for shock reflection computed order rotated difference method of Davis

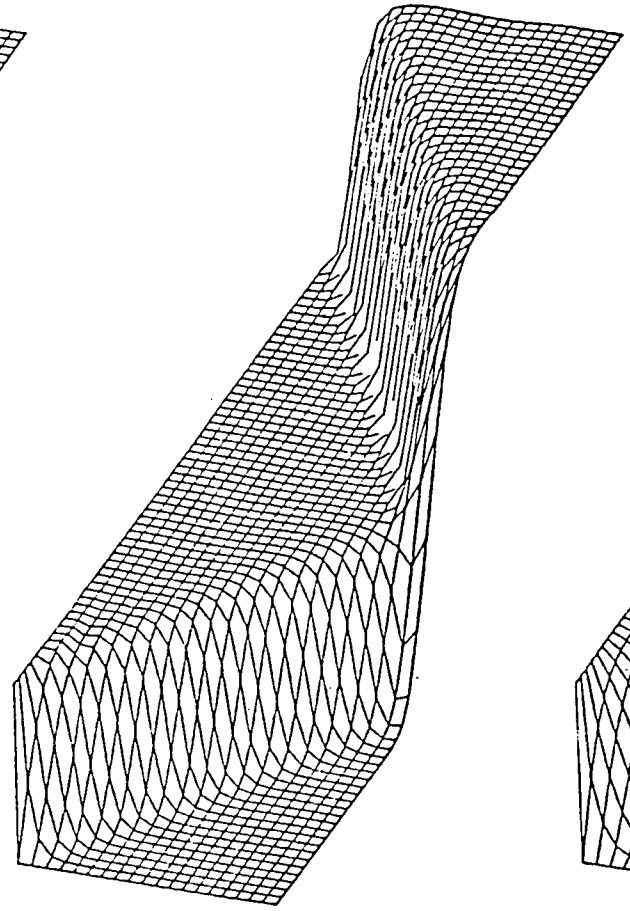

Figure 6 Three dimensional density plot for shock reflection computed using the second order method of van Leer

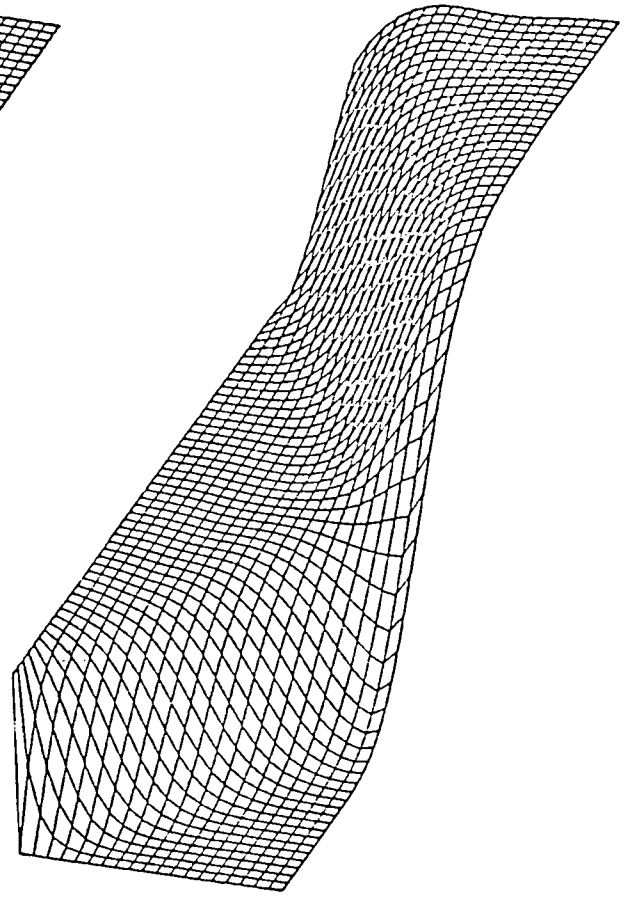

Figure 7 Three dimensional density plot for shock reflection computed using the first order method of Osher and Solomon

and a scheme is called total variation diminishing (TVD) if

$$TV(U^{n+1}) = TV(L.U^n) \leq TV(U^n). \tag{4.4}$$

In the following we consider only total variation diminishing schemes because solutions to TVD schemes do not exhibit spurious oscillations.

To determine whether a scheme is TVD, we rewrite it in the form

$$U_k^{n+1} = U_k^n - C_{k-1/2}\Delta U_{k-1/2}^n + D_{k+1/2}\Delta U_{k+1/2}^n \tag{4.5}$$

where

$$\Delta U_{k+1/2}^n = U_{k+1}^n - U_k^n \tag{4.6}$$

and $C_{k-1/2}, D_{k+1/2}$ are functions of U^n and we apply the following result.

Lemma (Harten). If the coefficients C and D of equation (5.4.5) satisfy the inequalities

$$\begin{aligned} &0 \leq C_{k+1/2} \\ &0 \leq D_{k+1/2} \\ &0 \leq C_{k+1/2} + D_{k+1/2} \leq 1, \end{aligned} \tag{4.7}$$

then the scheme (4.5) is TVD. ∎

There are a number of ways to construct TVD schemes. See the papers by Harten[3], Osher[6], Roe[9], and van Leer[13] for details of other approaches. Here we construct a scheme by adding a term of the form

$$K_{k+1/2}\Delta U_{k+1/2}^n - K_{k-1/2}\Delta U_{k-1/2}^n \tag{4.8}$$

to the Lax-Wendroff method

$$U_k^{n+1} = U_k^n - \frac{\nu}{2}(\Delta U_{k+1/2}^n + \Delta U_{k-1/2}^n) + \frac{\nu^2}{2}(\Delta U_{k+1/2}^n - \Delta U_{k-1/2}^n) \tag{4.9}$$

where $\nu = a\Delta t/\Delta x$ and K in equation (4.8) is chosen so that the resulting scheme is TVD.

If $a > 0$ and K is chosen to have the form

$$K_{k+1/2} = \frac{\nu}{2}(1-\nu)[1 - \phi(r_k^+)] \tag{4.10}$$

where

$$r_k^+ = \frac{\Delta U_{k-1/2}^n}{\Delta U_{k+1/2}^n} \tag{4.11}$$

and ϕ is the flux limiter, we obtain a scheme of the form (4.5) studied by Sweby[11]

$$\begin{aligned} C_{k-1/2} &= \nu\{1 + 1/2(1-\nu)[\phi(r_k^+)/r_k^+ - \phi(r_{k-1}^+)]\} \\ D_{k+1} &= 0. \end{aligned} \tag{4.12}$$

This scheme will be TVD provided $\nu < 1$ and

$$\frac{-2}{1-\nu} \leq [\phi(r_k^+)/r_k^+ - \phi(r_{k-1}^+)] \leq \frac{2}{\nu}\,. \tag{4.13}$$

If $a < 0$ and K is chosen to have the form

$$K_{k+1/2} = \frac{\nu(1+\nu)}{2}[\phi(r_{k+1}^-) - 1] \tag{4.14}$$

where

$$r_k^- = \frac{\Delta U_{k+1/2}^n}{\Delta U_{k-1/2}^n} \tag{4.15}$$

we obtain a scheme of the form (4.5) with

$$\begin{aligned} C_{k-1/2} &= 0 \\ D_{k+1/2} &= \nu\{-1 + 1/2(1+\nu)[\phi(r_{k+1}^-) - \phi(r_k^-)/r_k^-]\}. \end{aligned} \tag{4.16}$$

This scheme will be TVD provided $-\nu < 1$ and

$$\frac{-2}{1+\nu} \leq [\frac{\phi(r_k^-)}{r_k^-} - \phi(r_{k+1}^-)] \leq \frac{-2}{\nu}. \tag{4.17}$$

The schemes (4.12) and (4.16) can be combined into a single upwind scheme if K is chosen to have the form

$$K_{k+1/2} = \begin{cases} \frac{\nu}{2}(1-\nu) \quad [1 - \phi(r_k^+)]\,, & \text{if } a > 0 \\ \frac{\nu}{2}(1+\nu) \quad [\phi(r_{k+1}^-) - 1], & \text{if } a < 0 \end{cases} \tag{4.18}$$

For hyperbolic systems it would be convenient to have a method that did not require that we know which direction is upwind. To this end we rewrite (4.18) in the form

$$K_{k+1/2} = \frac{|\nu|}{2}(1 - |\nu|)[1 - \phi'(r_k^+, r_{k+1}^-)] \tag{4.19}$$

where ϕ' is an appropriately determined flux limiter. Roe[10] has done a considerable amount of work on what constitutes an appropriate flux limiter. In the remainder of this section we discuss this work.

In order to assure that the scheme (4.8), (4.9) is TVD, we require that inequalitites (4.13) and (4.17) hold. To simplify the analysis, we also require that $\phi > 0$ and $\phi = 0$ when $r < 0$. This reduces the scheme to first order in the vicinity of extrema and causes peaks to be "clipped." Attempts to correct these problems are the topics of current research. With these simplifications, inequalities (4.13) and (4.17) become

$$\phi(r_k^+) \leq min\left[\frac{2r_k^+}{\nu}, \frac{2}{1-\nu}\right] \tag{4.20}$$

and

$$\phi(r_k^-) \leq min\left[\frac{2r_k^-}{|\nu|}, \frac{2}{1-|\nu|}\right] \tag{4.21}$$

respectively.

Roe has shown that the scheme will be second order accurate if

$$\phi(r) = r + 0(1-r) \tag{4.22}$$

in the vicinity of $r = 1$. There is also a condition which assures that the method will be third order accurate, but it requires that the upwind direction be known so we will not discuss it here.

Of more interest is the limiter

$$\phi(r) = \frac{2r}{\nu(1-\nu)} \frac{(1-r^\nu) - \nu(1-r)}{(1-r)^2} \tag{4.23}$$

derived by Roe which exactly convects exponentially varying data. Although this limiter which Roe calls Hyperbee, is too complex and does not perform well in practice, it seems to provide a yardstick for choosing good limiters. In particular, Roe's numerical experiments seem to show that any limiter which crosses Hyperbee in two places other than $r = 1$ will convect step data as a smooth profile which does not spread with time. This is an exciting result since all other schemes are known to spread step data.

A closer look at these results shows that this smooth profile consists of two exponentials, corresponding to those values of r where the limiter crosses Hyperbee, connected by a smooth curve that does not grow in time. Recently, this author has constructed mathematical proofs of some of these results.

Figure 8 is a sketch of the Hyperbee limiter and the upwind limiter

$$\phi(r) = max\left[0, min\left(\frac{2r}{|\nu|}, 1\right), min\left[r, \frac{2}{1-|\nu|}\right)\right] \tag{4.24}$$

which Roe calls Ultrabee. Figure 9 shows the results of a computation using the Ultrabee limiter to convect a square wave for 250 time steps at a Courant number

of 0.5. Figure 10 shows the results of this same computation using the non-upwind limiter

$$\phi'(r^+, r^-) = max[0, min(\frac{2r^+}{|\nu|}, r^-, \frac{2}{1-|\nu|}), min(\frac{2r^-}{|\nu|}, r^+, \frac{2}{1-|\nu|})]. \qquad (4.25)$$

These figures show that the upwind limiter gives sharper steps but the non-upwind limiter still gives acceptable results. The upwind limiter is able to satisfy more closely the inequalitites (4.20), (4.21) and this is the reason for its better performance. On the other hand, the non-upwind limiter is simple to program and would probably run faster than the upwind limiter.

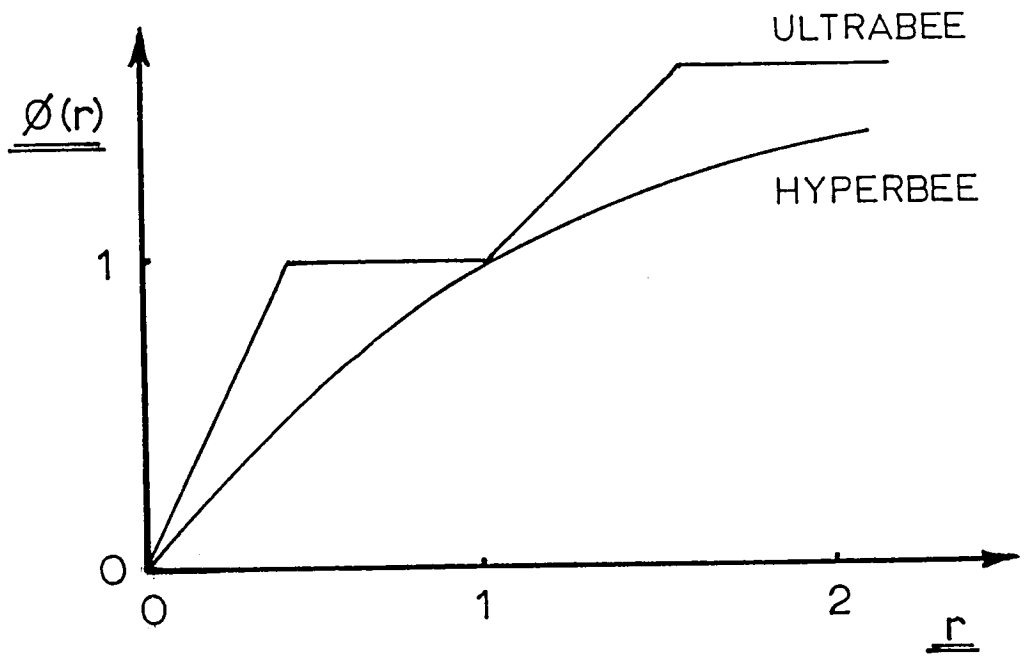

Figure 8. Flux limiters.

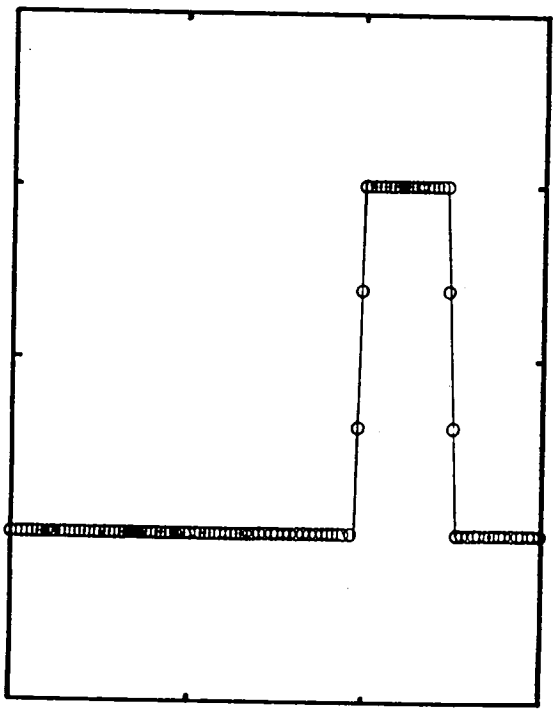

Figure 9. Linear advection of a square pulse computed using the MacCormack scheme and the upwind Ultrabee limiter.

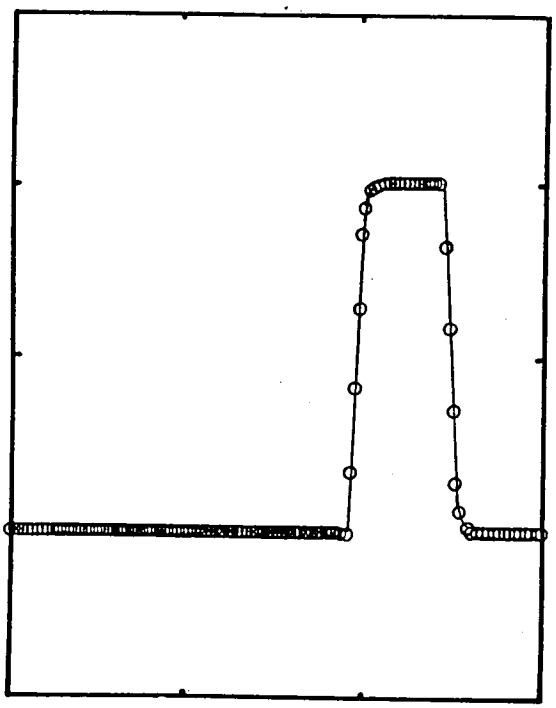

Figure 10. Linear advection of a sqaure pulse computed using MacCormack scheme and the non-upwind limiter equation (4.25).

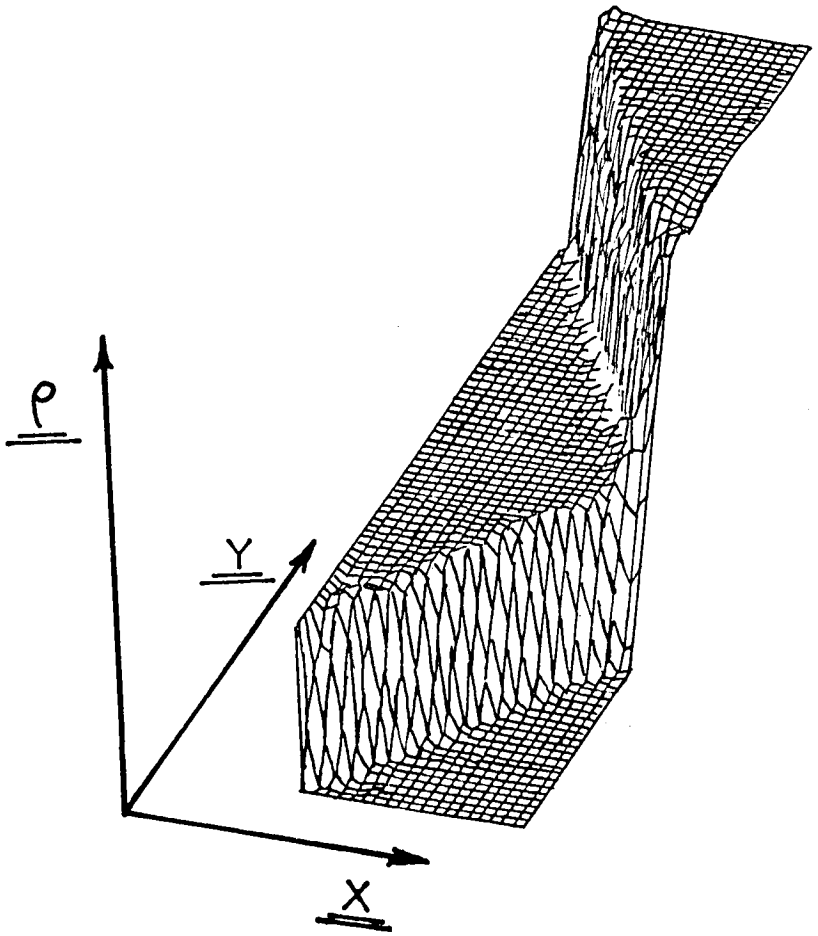

Figure 11. Three dimensional density plot for shock reflection computed using the MacCormack scheme and the non-upwind limiter equation (4.25).

Figure 11 shows results of the application of the non-upwind limiter to the shock reflection problem. We believe that the standing waves along the reflected shock are due to the treatment of the wall boundary conditions or to the way that we extended our one dimensional results to two dimensions. This is currently being investigated.

5.6 Summary

In this chapter we have examined how upwind differencing and flux limiters improve the resolution of numerical approximations to discontinuous solutions of hyperbolic systems. The study of these numerical processes has led to the development of new numerical methods of high accuracy which resolve shocks without excessive spreading or spurious wiggles.

Here we have concentrated on three special cases. In particular we showed

how the requirement that a finite difference scheme be conservative is equivalent to the requirement that some pointwise error be made in the vicinity of a shock. On the other hand a properly constructed upwind difference scheme will confine these errors to one mesh interval if the shock is steady. This result has been applied to one dimensional problems for some time. Here we also showed how to apply it to two dimensional problems.

For moving discontinuties, it is well known that the use of flux limiters permits the construction of high order upwind schemes which can resolve these discontinuities without spurious wiggles. Here we have shown that this construction can also be applied to second order central difference schemes and that the resulting schemes are simpler than their upwind counterparts.

Finally, we have described an exciting discovery by P. L. Roe. Roe has characterized a class of flux limiters which are observed experimentally to approximate a discontinuity by a smooth narrow transition that does not spread as it is advected. So far as we know all other schemes spread linear discontinuities for all time.

References

1.) **Davis, S. F.**, "A Rotationally Biased Upwind Difference Scheme for the Euler Equations," J. Comp. Phys., 56 (1984), pp. 65-92.

2.) **Davis, S. F.**, "TVD Finite Difference Schemes and Artificial Viscosity," ICASE Report 84-20, NASA CR-172373, 1984.

3.) **Harten, A.**, "High Resolution Schemes for Hyperbolic Conservation Laws," J. Comp. Phys., 49 (1983), pp. 357-393.

4.) **Lax, P. and Wendroff, B.**, "Systems of Conservation Laws," Comm. Pure Appl. Math., 13 (1960), pp. 217-237.

5.) **Murman, E. M.**, "Analysis of Embedded Shock Waves Calculated by Relaxation Methods," AIAA J., 12 (1974), pp. 626-633.

6.) **Osher, S. and Chakravarthy, S.**, "Very High Order Accurate TVD Schemes," ICASE Report 84-44, 1984.

7.) **Osher, S. and Solomon, F.**, "Upwind Difference Schemes for Hyperbolic Systems of Conservation Laws," Math. Comp., 38 (1982), pp. 339-374.

8.) **Roe, P. L.**, "Approximate Riemann Solvers, Parameter Vectors and Difference Schemes," J. Comp. Phys., 43 (1981), pp. 357-372.

9.) **Roe, P. L.**, "Fluctuations and Signals, a Framework for Numerical Evolution Problems," in *Numerical Methods for Fluid Dynamics*, K. W. Morton and M.

J. Baines (eds.), Academic Press, 1982.

10.) **Roe, P. L.**, "Some Contributions to the Modelling of Discontinuous Flows," Proceedings AMS/SIAM Summer Seminar on Large Scale Computations in Fluid Mechanics, 1983, to appear.

11.) **Sweby, P. K.**, "High Resolution Schemes using Flux Limiters for Hyperbolic Conservation Laws," SIAM J. Num. Anal., 21 (1984), pp. 995-1011.

12.) **van Leer, B.**, "Flux Vector Splitting for the Euler Equations," ICASE Report 82-30, 1982.

13.) **van Leer, B.**, "Computational Methods for ideal Compressible Flow," ICASE Report 83-38, NASA CR-172180, 1983.

1. Report No. NASA CR-172592 ICASE Report No. 85-25	2. Government Accession No.	3. Recipient's Catalog No.
4. Title and Subtitle Shock Capturing		5. Report Date April 1985 6. Performing Organization Code
7. Author(s) Stephen F. Davis		8. Performing Organization Report No. 85-25
9. Performing Organization Name and Address Institute for Computer Applications in Science and Engineering Mail Stop 132C, NASA Langley Research Center Hampton, VA 23665		10. Work Unit No. 11. Contract or Grant No. NAS1-17070
12. Sponsoring Agency Name and Address National Aeronautics and Space Administration Washington, D.C. 20546		13. Type of Report and Period Covered Contractor Report 14. Sponsoring Agency Code 505-31-83-01
15. Supplementary Notes Langley Technical Monitor: J. C. South, Jr. Final Report		To appear in Numerical Methods for Partial Differential Equations, S.I. Hariharan and T.H. Moulden (eds.), Pitman, 1986.

16. Abstract

This chapter describes recent developments which have improved our understanding of how finite difference methods resolve discontinuous solutions to hyperbolic partial differential equations. As a result of this understanding improved shock capturing methods are currently being developed and tested. Some of these methods are described and numerical results are presented showing their performance on problems containing shocks in one and two dimensions.

We begin this discussion by defining what is meant by a conservative difference scheme and showing that conservation implies that, except in very special circumstances, shocks must be spread over at least two grid intervals. These two interval shocks are actually attained in one dimension if the shock is steady and an upwind scheme is used. By analyzing this case, we determine the reason for this excellent shock resolution and use this result to provide a mechanism for improving the resolution of two-dimensional steady shocks. Unfortunately, this same analysis shows that these results cannot be extended to shocks which move relative to the computing grid.

To deal with moving shocks and contact discontinuities we introduce total variation diminishing (TVD) finite difference schemes and flux limiters. We show that TVD schemes are not necessarily upwind, but that upwind TVD schemes perform better because they permit a wider choice of flux limiters. The advantage of non-upwind TVD schemes is that they are easy to implement. Indeed, it is possible to add an appropriately chosen artificial viscosity to a conventional scheme such as MacCormack's method and make it TVD. We conclude by presenting some theoretical results on flux limiters and some numerical computations to illustrate the theory.

17. Key Words (Suggested by Author(s))	18. Distribution Statement
hyperbolic partial differential equations, shock waves, finite difference methods	64 - Numerical Analysis Unclassified - Unlimited

19. Security Classif. (of this report)	20. Security Classif. (of this page)	21. No. of Pages	22. Price
Unclassified	Unclassified	23	A02

For sale by the National Technical Information Service, Springfield, Virginia 22161

NASA-Langley, 1985